High resolution desktop micro computed tomography for the evaluation of reducing treatments on historical glass suffering from manganese browning

RESEARCH · MARCH 2016

READS
2

7 AUTHORS, INCLUDING:

Jakub Jaroszewicz
Warsaw University of Technology
64 PUBLICATIONS **332** CITATIONS
SEE PROFILE

Hilde Wouters
Vrije Universiteit Brussel
20 PUBLICATIONS **160** CITATIONS
SEE PROFILE

Joost M. A. Caen
University of Antwerp
35 PUBLICATIONS **117** CITATIONS
SEE PROFILE

Koen Janssens
University of Antwerp
392 PUBLICATIONS **5,381** CITATIONS
SEE PROFILE

High-resolution Desktop Microcomputed Tomography for the Evaluation of Reducing Treatments on Historical Glass Suffering From Manganese Browning

Gert Nuyts,* Simone Cagno, Jakub Jaroszewicz, Hilde Wouters, Kristel De Vis, Joost Caen, Koen Janssens
*Corresponding author

Keywords:
manganese browning; manganese intrusion; desktop microcomputed tomography; reducing treatment

Abstract
Historical glass, especially non-durable mediaeval glass, can undergo corrosion. This sometimes results in the formation of dark-coloured manganese-rich inclusions or stains that reduce the transparency of the glass. A conservation treatment with reducing or chelating agents may be considered with the aim of improving the transparency. In this paper, high-resolution desktop microcomputed tomography (μCT) is used in combination with element-specific two-dimensional imaging methods for in situ monitoring of manganese removal by hydroxylamine hydrochloride from an archaeological stained-glass sample suffering from manganese browning and from artificially corroded model glass samples. μCT also proved itself useful for the study of the (re-)penetration of manganese into the gel layer during artificial corrosion of a model glass.

Introduction
Glass, including window panes from existing stained-glass windows or fragments encountered in an archaeological context (e.g. at excavations of church sites, monastery sites), is often affected by so-called darkening or browning caused by the development of dark-coloured Mn/Fe-rich zones in the alteration layer; sometimes this can lead to a reduced or total loss of transparency of the glass. This phenomenon has been reported in the literature for archaeological glass excavated from different northern European sites situated in, for example, Belgium, Spain and the U.K. and dating from the 11th to the 16th century (Newton and Davison 1989; Schreiner 1991; Müller, Torge, and Adam 1994; Müller, Torge, and Adam 1995; Watkinson, Weber, and Anheuser 2005; Doménech-Carbó and others 2006; Cagno and others 2011; Schalm and others 2011; Wouters 2013). In this paper, the focus of attention is on the darkening caused by Mn-rich zones or plugs (Roemich and others 2003), henceforth referred to as Mn inclusions (Doménéch-Carbó, Doménéch-Carbó, and Osete-Cortina 2001), and how high-resolution microcomputed tomography (μCT) can be used to explore their formation and treatment.

While this study deals with both the removal and artificial intrusion of Mn staining, it is important to point out that the main objective of a glass conservator (based upon internationally accepted guidelines) is the conservation of original (glass) material and the prevention of further decay with minimal intervention. This objective would generally not include the recovery of the transparency of Mn-darkened glass fragments through the removal of corrosion products and deposits. Corrosion products are considered to be a part of the material history of a sample and thus a part of its cultural value (Corpus Vitrearum, Guidelines for the Conservation and Restoration of Stained Glass 1.3, 2nd edition, Nuremberg, 2004). To appreciate the highly fragmented state of archaeological glass collections, it is important to understand their lifespan through the interpretation of signs of production, design, use, re-use, repair and deposition of such fragments in relation to their specific context (Wouters 2013). For glass, any loss of the corrosion layers results in a

loss of technological traces and, therefore, a loss of information (Wouters 2013). Any intervention should be reversible and non-destructive. However, a non-reversible treatment method may be considered in a limited number of cases, e.g. in extreme cases of darkening where the original colour of the glass and other signs of its history such as applied paint or design on the surface can no longer be appreciated.

Two different strategies are known to conservators for removing the darkening effect induced by manganese: one is based on the reduction of the highly oxidised black/brown compounds, and the other focuses more on the extraction of this element from the inclusions by means of the application of chelating agents (Fitz 1981; Newton and Davison 1989). The heterogeneity of degraded historical glass (Newton and Davison 1989) makes it difficult to compare different methods of treatment, since historical glass exhibits a large range of weathering phenomena (Newton and Davison 1989) and has a variable composition, while its corrosion history is in many cases unknown. Samples with identical initial properties are rarely available. This can be circumvented by testing treatments on model glass samples, which may be artificially corroded to simulate phenomena encountered on original glass fragments; this allows full control over the composition of the glass and the parameters of the artificial corrosion process in order to ensure the reproducibility of such experiments. Additional reasons for preparing synthetically corroded glass are (a) that it is ethically appropriate to use such material in order to avoid damaging historical glass fragments during comparative tests and (b) that a systematic study of the phenomena taking place during glass corrosion and/or its treatment may expand our knowledge on the manganese browning phenomenon and the factors that govern it.

In some cases, evaluation of conservation measures requires high-resolution analytical techniques appropriate to detect the degradation phenomena and the subtle changes that may occur to the glass during treatment. µCT has already proven its usefulness for the characterisation of degraded glass (Lopez and others 2002; Roemich and others 2003; Mees and others 2009; Schalm and others 2011). By employing the local density contrast, a 3D image can be obtained in which not only the position and volume of (internal) cracks and voids in the glass may be visualised but also the size and shape of the Mn inclusions may be determined. Schalm and others (2011) describe the presence of dendrites and of planar- and tubular-shaped enrichments inside the gel layer. These findings allowed them to formulate the hypothesis that such inclusions are formed by migration of Mn(II) towards the inclusions, followed by in situ oxidation.

In order to assess the effect of a reducing treatment on existing Mn stains or of a treatment intended to induce the artificial formation of such stains, the glass material in which these transformations take place needs to be compared before and after treatment. While µCT is very useful to determine the 3D morphology of the Mn inclusions, it suffers from the limitation of being not element-specific. In what follows, we therefore use µCT either in combination with scanning electron microscopy-energy dispersive X-ray spectrometry (SEM-EDX), a conventional analytical method frequently employed to study glass degradation (Janssens and Van Grieken 2004), or together with microscopic X-ray fluorescence analysis (µXRF), a more sensitive equivalent of SEM-EDX. These methods require polished cross-sections to be prepared from the samples, making it more difficult to study changes before, during and after treatment.

In a previous study on manganese browning, microscopic high-resolution synchrotron-radiation-based CT (µSR-CT) was used to evaluate the effect of a hydroxylamine hydrochloride ($NH_2OH{\cdot}HCl$) treatment of glass. Glass fragments with a comparable provenance as the materials employed here were immersed in a 2–5 wt% $NH_2OH{\cdot}HCl$ solution. At a spatial resolution level of 0.7 µm, it could be demonstrated that not only was Mn in inclusions (assumed to be present as MnO_2) reduced to the water soluble Mn(II) form (Cagno and others 2011), but also the enhanced mobility (Watkinson, Weber, and Anheuser 2005) of the Mn allowed it to diffuse into the treatment solution, thus removing it from the gel layer (Cagno and others 2011). While µSR-CT allows one to distinguish between the original glass, the gel layer and the Mn inclusions, another advantage of the SR variant is its speed: by exploiting a total scan time of approximately 10 minutes, it was possible to monitor the gradual removal of the Mn resulting from a series of short exposures to the treatment solution (Cagno and others 2011). An important restriction of µSR-CT, on the other hand, is the limited availability of experimental time at large-scale synchrotron facilities. A relevant question in this context is, therefore, to what extent a high-resolution desktop mCT apparatus may be used for the above-mentioned type of investigations.

Accordingly, in this paper, we first describe the results of a comparative study between desktop and SR-based mCT conducted on an expendable historical glass fragment showing manganese staining; SEM-EDX was employed to map the presence of this element. The sample was characterised in 3D

before and after treatment with a 5 wt% $NH_2OH{\cdot}HCl$ solution, intended to reduce and remove the Mn from the glass. Second, in combination with µXRF, high-resolution desktop µCT was used to study the phenomenon of Mn intrusion from a solution into the glass gel layer during artificial degradation. More specifically, these methods were used to verify whether Mn intrusion and precipitation occurs only in the microscopic cracks of a pre-corroded non-durable glass fragment or whether Mn(II) effectively penetrates into the gel layer, as suggested by Schalm and others (2011).

Background on Manganese Browning

Glass Corrosion

In general, corrosion of historical silicate glass (Roemich and others 2003) is induced by the presence of water: molecular water penetrates into the glass via diffusion and/or reversible hydrolysis/condensation reactions. As a result, the silica network will undergo structural transformations (Bunker 1994). Simultaneously, an ion-exchange process will take place, mainly at low pH values, between protons from the environment and cations present within the glass network (Scholze 1982; Janssens and others 1996; Adams and others 1997; Melcher and Schreiner 2004). This results in leaching out of most mobile cations (i.e., monovalent Na^+ and K^+), during which the density of the gel layer will decrease, since heavier metal cations are being replaced by lighter protons and water. If the surface of the glass is subject to dry/wet cycles, microcracks can occur, leading to the formation of very thin (< 1 µm) lamellae (Schalm and others 2011). In addition, weathering products (such as sulfates and chlorides of Mg or Ca) can be formed on the glass surface (Roemich and others 2003; Doménech-Carbó and others 2006). If the original glass contains Mn, this element can also become depleted in the gel layer (Janssens and others 1996).

Manganese Browning

As described elsewhere in more detail (Schalm and others 2011), when an internal or external manganese source is available, Mn inclusions can be formed within the leached layer. Historical glass often contains a small amount of manganese (typically 0.5–1 wt%) with Mn(II) being the predominant species. Manganese can be present in the glass as an impurity of the starting materials or can have been added deliberately as pyrolusite (MnO_2), a de-colourising agent (Newton and Davison 1989). Alternatively, manganese may be introduced into archaeological glass from the soil in which the glass was buried (Cox and Ford 1993; Doménech-Carbó, Doménech-Carbó, and Osete-Cortina 2001). Previous experiments have indicated the presence of MnO_2 in the Mn inclusions (Schalm and others 2011), and a hypothesis for its formation was proposed: in the presence of water and oxygen, Mn(II) and/or Mn(III) ions can be oxidised to higher oxidation states, giving rise to, for example, insoluble MnO_2 from which the Mn inclusions are formed (Doménech-Carbó, Doménech-Carbó, and Osete-Cortina 2001; Cagno and others 2011; Schalm and others 2011). Manganese inclusions are sometimes referred to as 'corrosion bodies' (Cagno and others 2011; Schalm and others 2011).

Experimental

Microcomputed Tomography

X-ray absorption tomography is a non-destructive technique that allows 3D visualisation of the linear attenuation coefficient, which is equal to the product of the local mass absorption coefficient and density (Sasov and Van Dyck 1998). The 3D images generated by µCT consist of slices, where each slice corresponds to a virtual cross-section of the sample. In each slice, the grey value represents the linear attenuation in that specific location.

Two different lab µCT scanners were used to image the corroded glass fragments, namely a Skyscan 1172 high-resolution micro-CT and an Xradia MicroXCT-400 instrument. The first is equipped with a Hamamatsu 100 kV tungsten X-ray source and an 11 Mp Skyscan CCD camera. The Xradia has a Hamamatsu 150 kV X-ray source and a 2 K x 2 K Andor CCD camera. In addition to the geometric magnification, the Xradia also includes a set of scintillator-coated objective lenses with an optical magnification of 0.5x, 4x, 10x, 20x and 40x, which allow better resolution than the Skyscan 1172. All measurements using the Skyscan 1172 were carried out with an operating acceleration voltage of 70 kV and a source current of 139 µA. A 0.5 mm Al filter was inserted in the incoming beam in order to remove the soft X-rays. These cannot pass through the sample and do not contribute to the acquired radiograph, but their scattering can still induce noise and unnecessary sample heating. Only one glass fragment was measured using the high-resolution

Sample	Scanner	Treatment	μCT parameters				
			Exposure time/ angle	Rotation step (°)	Total rotation angle (°)	Image pixel size (μm)	Total scan duration (hours)
Sample A	Skyscan 1172	30 min 5 wt% $NH_2OH{\cdot}HCl$	300 ms	0.150	360	4.2	± 4.5
Sample B Fraunhofer M1.0	Skyscan 1172	2 h 1 M HCl	500 ms	0.4	360	3.05	± 2
Sample C Fraunhofer M1.0	Skyscan 1172	2 h 1 M HCl + 24 h 0.5 M $MnCl_2$	780 ms	0.3	192	2.4	± 2
Sample D Fraunhofer M1.0	Xradia XCT-400	2 h 1 M HCl + 24 h 0.5 M $MnCl_2$	10 s	0.072	180	1.1	± 17 h

Table 1. Summary of the treatments applied to the glass samples and the instrumental parameters used during μCT acquisition.

Xradia instrument employing a 50 kV acceleration voltage and a 200 μA current. Reconstructions were performed using an algorithm based on cone beam filtered back projection, including ring-artefact and beam-hardening corrections. The latter is required since a polychromatic primary beam is used. Other experimental parameters are unique for every measured glass fragment and are summarised in table 1; this table also summarises all the chemical treatments employed.

Reducing Treatment of Historical Glass

Sample A, used to compare SR-CT with desktop μCT, is part of a series of glass fragments that originate from an excavation at a former Franciscan friary and are dated to the 14th century. Since the context data of the excavation were lost, the heritage value of this fragment is limited (Hind, Marsden, and Evans 1994). The major components (wt%) of the original glass in sample A were determined by SEM-EDX analysis:[1] MgO 5.2%; Al_2O_3 2.0%; SiO_2 46.8%; K_2O 18.4%; CaO 23.6%; and MnO 1.6%. The relatively large size (around 1 mm depth and around 2 mm width) of the dark Mn-enriched zone at the original glass surface makes this sample very suitable for the μCT comparison study. In order to obtain optical microscopy images from this sample before and after $NH_2OH{\cdot}HCl$ treatment, the glass sample was embedded in Versocit-2 acrylic resin and consecutively cut and polished. Embedding also helped to preserve sample integrity during diamond saw cutting.

The reducing treatment involved immersing the embedded glass sample for 30 min in a 5 wt% $NH_2OH{\cdot}HCl$ aqueous solution. The same concentration as employed in the SR-CT study was used; there, this relatively high concentration was chosen in order to accelerate the treatment effect and to allow for a series of short exposures to the $NH_2OH{\cdot}HCl$ alternated with SR-CT data acquisition (Cagno and others 2011). Also in this case, immersion in this solution results in consecutive Mn reduction and removal. An important difference between these experiment and 'real' treatments performed by glass conservators can be noted with respect to the contact surface of the glass fragment with the treatment solution. In the present experiment, a cross-sectional plane of the sample (figure 1(c)) was exposed to the reducing solution, while the original (naturally corroded) surface of the glass fragment was shielded by the embedding resin; during an actual conservation treatment, the solution would be in contact with the original surface.

Artificial Degradation

Fraunhofer type M1.0 sensor glass (54.2 wt% SiO_2, 28.8 wt% K_2O, 17.0 wt% CaO) (Fuchs, Roemich, and Schmidt 1991) was used as starting material for the artificial alteration. A two-step treatment was employed to realise a rapid weathering/staining process. Fragments of type M1.0 glass were immersed consecutively in 1 M HCl (2 hours) and 0.5 M $MnCl_2$ solutions (24 hours). The immersion in acid leads to the creation of a leached/hydrated layer, while immersion in the $MnCl_2$ solution introduces Mn into the gel layer.

Results and Discussion

Desktop μCT Imaging of a Reducing Treatment

A schematic overview of the orientation of original bulk glass, gel layer and Mn inclusions of sample A is shown in figure 1(a). Figure 1(b) shows a Mn elemental distribution map of part of the area obtained by SEM-EDX,[2] indicating

that Mn-rich inclusions of lateral dimension 10–20 µm are present. On the optical microscope image prior to treatment (figure 1(c)), a gel layer (in grey) can be observed on both outer surfaces of the glass fragment with black Mn inclusions inside. (The purple regions that can be observed on the left side of the sample in figure 1(c) are a flashed glass layer.) Figure 1(d) shows a microphotograph of sample A after the treatment. In figure 2, tomograms of the left Mn stain of figure 1(c) are shown, obtained by µCT before (figures 2(a) and (c)) and after (figures 2(b) and (d)) the reducing treatment. The large dimensions of the Mn inclusions (figure 1(b)) allowed the lower resolution settings (4.2 µm) of the Skyscan 1172 system to be used, making it possible to visualise a larger volume (see table 1 for a summary of all operating parameters).

A comparison of the images in figures 1(c) and (d) shows that, already after 30 min of exposure, the damage to the bulk glass caused by the treatment can be observed; the surface has developed a crack pattern, resulting in increased light scattering. A second observation is that the browning effect has partially disappeared; this indicates that some manganese, originally present in the +IV state of oxidation, was reduced in accordance with the results obtained by Cagno and others (2011). However, some residual bluish-grey coloured zones can still be observed inside the gel layer, suggesting that not all oxidised Mn has been removed.

While one tomographic scan using SR-CT required approximately 10 minutes, by means of the desktop µCT, a total of 4.5 hours of measurement time was needed. Thus, it was only possible to evaluate the reducing treatment in a before/after fashion without recording of 3D data at the intermediate stages. The tomograms shown in figures 2(a) and (b) correspond to the contact surface, while the slices in figures 2(c) and (d) are situated around 40 µm below the surface. More dense areas are represented by lighter grey values, and less dense areas are represented by by darker values. Accordingly, the less dense gel layer appears darker grey in the CT image than the bulk glass. Due to a higher local density, Mn inclusions show up brighter than the surrounding gel layer. At the surface (figures 2(a) and (b)), a significant fraction of the Mn has disappeared during the 30-minute exposure to the reducing solution; however, at 40 µm below the surface (figures 2(c) and (d)), this is far less the case.

When comparing SR-CT and desktop CT, it can be noted that the desktop CT employed here has sufficient resolution and contrast to make the distinction between the various phases in the corroded glass and to observe relevant changes inside the material when it is exposed to the reducing solution. The long data acquisition time required by the desktop instruments, however, makes it not practical to record many intermediate stages during a treatment of this kind. From the images shown in figure 2, it can be concluded that, after 30 minutes of exposure, the influence of the $NH_2OH{\cdot}HCl$ solution is fairly superficial only.

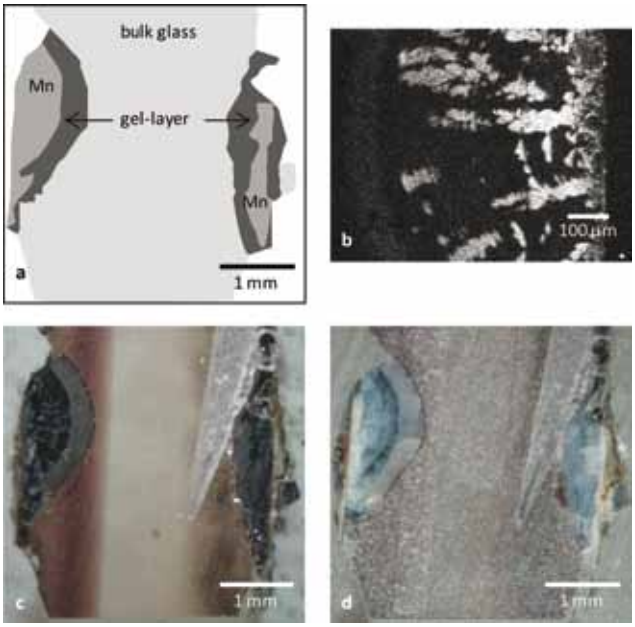

Fig. 1. Sample A prepared as cross-section: schematic overview (a); elemental distribution map of Mn, obtained with SEM-EDX (b); optical microscopy image, before treatment (c); optical microscopy image, after 30-minute treatment with 5 wt% $NH_2OH{\cdot}HCl$ solution (d) (Images: the authors).

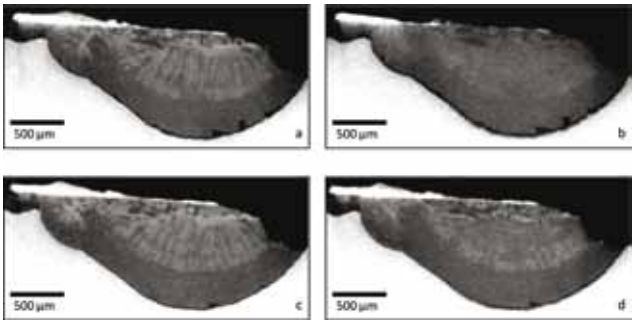

Fig. 2. Virtual slices of sample A obtained by means of desktop µCT: at the surface of the cross-section of the embedded fragment, before (a) and after 30 min treatment with 5 wt% $NH_2OH{\cdot}HCl$ solution (b); parallel slice at around 40 µm below the surface, before (c) and after treatment (d) (Images: the authors).

Gert Nuyts, Simone Cagno, Jakub Jaroszewicz, Hilde Wouters, Kristel De Vis, Joost Caen, Koen Janssens

Microcomputed Tomography on Model Glasses: Detecting Artificial Corrosion Layers

The optical photographs shown in figures 1(c) and (d) underline that chemical treatment methods for glass can induce unwanted damage; this makes it questionable to use historical glass fragments in optimisation experiments for conservation methods, especially considering the art-historical value of most fragments.

During previous experiments on artificial glass alteration, it was already demonstrated that Mn intrudes into the gel layer (Nuyts and others 2013). Figure 3(a), obtained by μXRF[3] from a cross-sectioned sample of Fraunhofer M1.0 glass treated with HCl and $MnCl_2$, shows that this preferentially takes place via microscopic cracks that have formed during the exposure to HCl (figure 3(b)). It was previously shown that Mn_3O_4 is the dominant Mn species (Nuyts and others 2013), without any significant spatial variation or any variation with treatment time, causing the typical brownish-black colour (Hao and others 2011). The specific advantage of μCT here is that glass fragments can be studied at and below the exposed surface without the necessity to prepare exposed, polished cross-sections of the sample and thus without the risk of removing intruded Mn during such preparation.

Figures 3(c) and (d) show virtual cross-sections of the gel layer, 14–15 μm below the original glass surface, after treatment of M1.0 sensor glass with both the HCl and $MnCl_2$ solutions (sample C). The dark grey colour visible in almost the entire slice corresponds to the gel layer, having a density lower than that of the original bulk glass. When sample C was analysed using the Skyscan 1172 instrument (using the conditions given in table 1), a series of virtual slices with around 2.4 μm resolution were obtained. At the top of the tomographic slice shown in figure 3(c), which is not perfectly parallel to the outer surface of the fragment, the denser bulk glass is visible. Inside the gel layer, some brighter areas/lines, corresponding to a higher density material, can be observed. These areas correspond to the cracks visible in figure 3(a), where a local enrichment and the higher density is caused by local precipitation of Mn. Without the $MnCl_2$ treatment (sample B), the cracks are also visible in the tomograms, but then as areas of lower density (dark lines in figure 3(b)). Thus, the combined μXRF and μCT images suggest that Mn has indeed penetrated the cracks created by the HCl treatment.

In order to ascertain whether the Mn only filled up the cracks or actually penetrated the gel layer, glass sample D (a duplicate of sample C) was analysed at higher resolution by using the Xradia instrument (resolution of around 1 μm; see table 1 for the data-acquisition parameters). A virtual cross-section parallel to the original glass surface within the gel layer is shown in figure 3(d). Similar to the image shown in figure 3(c), Mn enrichments can be observed as brighter areas in the grey-coloured gel layer. In this image (figure 3(d)), also some unfilled cracks (dark lines across the gel layer) are present. More importantly, however, inside the bright areas, a slightly darker core can be observed, representing the original, physical cracks in the material. From this observation, we tentatively deduce that Mn effectively enters the material via the cracks previously created by the HCl treatment and, from there, diffuses into the silicon–oxygen network of the gel layer. The μXRF elemental distribution maps (figure 3(a)) do not provide enough resolution to visualise this effect.

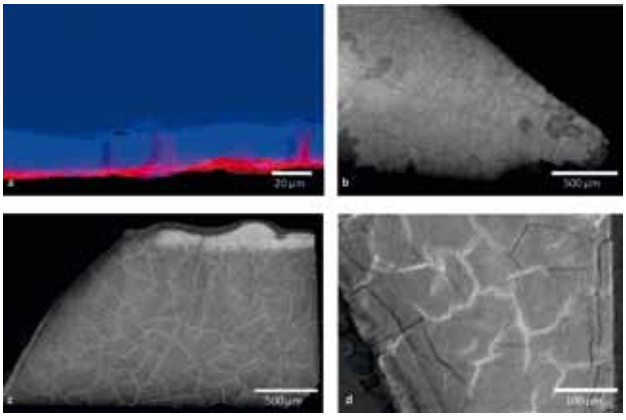

Fig. 3. (a) Si (blue) and Mn (red) elemental distribution maps of a cross-section of an artificially altered model glass sample, obtained with μXRF; (b) virtual slices of model glass samples obtained with μCT, around 10 μm below the original glass surface after a 2-hour HCl treatment (sample B, medium resolution Skyscan 1172 data); (c) around 14 μm below the original glass surface after consecutive HCl and $MnCl_2$ treatment (sample C, medium resolution Skyscan 1172 data); and (d) around 15 μm below the original glass surface (sample D, higher resolution Xradia XCT-400 data) (Images: the authors).

Conclusions

In the first part of this paper, the treatment of historical glass suffering from manganese browning with $NH_2O{\cdot}HCl$ was investigated: the applicability of desktop μCT for in situ monitoring of chemical changes was compared to that of the synchrotron-radiation-based equivalent.

Using a medium resolution desktop µCT instrument (Skyscan 1172), a behaviour in accordance with the results previously obtained by Cagno and others (2011) using µSR-CT was observed, where consecutive Mn reduction and removal was demonstrated. However, the relatively long scan times of the desktop system did not allow quasi-continuous monitoring of the treatment effects. On the positive side, the desktop variant does not suffer from the limited availability of SR-CT facilities and could therefore be used for in situ monitoring of slower-acting, and therefore more realistic, conservation procedures of this type, albeit with a coarser time resolution (i.e. of the order of days rather than of hours).

In the second part of the paper, desktop µCT was proven to be useful for determining how Mn may be introduced into the gel layer formed during artificial corrosion of glass samples of low durability (Fraunhofer M1.0). Previous experiments associated visual browning of the altered glass with the precipitation of Mn in the gel layer as brownish-black Mn_3O_4. This could also be observed by medium-resolution desktop CT. In high-resolution scans (1.1 µm), indications suggesting the diffusion of Mn from the microcracks into the surrounding gel layer could be observed. This will need to be investigated in greater detail by means of an element specific method such as high-resolution XRF tomography or transmission electron microscopy coupled to EDX.

The two-step artificial corrosion, described in this paper, was performed to induce manganese browning in a relatively short time period (around 26 hours), making it possible to evaluate the applicability of desktop µCT. However, gel layers produced by immersion in acidic solutions are different compared to degradation layers of glass fragments buried in the soil. Thus, in a next step, a less aggressive form of artificial corrosion will be evaluated. Another parameter to change is the composition of the substrate. In this study, highly sensitive M1.0 Fraunhofer glass without Mn was used together with an external Mn source. To better match realistic conditions in future experiments, the artificial corrosion will be performed on Mn-containing glass, allowing browning on glass with an internal Mn source to be simulated, as described by Roemich and others (2003). In both cases, high-resolution desktop µCT in combination with an element-specific imaging method will be used to visualise the Mn distribution before and after treatment in order to compare different methods applicable to conservation practice.

Acknowledgements

This research was supported by the Interuniversity Attraction Poles Programme – Belgian Science Policy (IUAP VI/16). The text also presents results of GOA 'XANES meets ELNES' (Research Fund University of Antwerp, Belgium) and from the Fund for Scientific Research (FWO, Brussels, Belgium) projects no. G.0704.08 and G.01769.09. All CT analyses were performed at the Department of Materials Science and Engineering of Warsaw University of Technology, and SEM-EDX mapping was performed in collaboration with Mr N. Lousberg from the EMAT research group of the Department of Physics of the University of Antwerp.

The authors also want to thank Leonie Seliger of Canterbury Cathedral, U.K., the Sidney Sussex College Council and Bursar Charles Larkum for providing the archaeological samples of the Franciscan Friary, which are kept in store for Sidney Sussex College in Cambridge (U.K.).

Notes

1. Quantitative analysis was performed using a JEOL 6300 scanning electron microscope equipped with an energy dispersive X-ray detector. Spectra were collected for 200 seconds using a 2 nA electron beam current, an accelerating voltage of 20 kV and a microscope magnification of 500. The net intensities were calculated with the program AXIL (Analysis of X-rays by Iterative Least squares) and quantified by means of a standardless ZAF program.
2. The X-ray map was recorded using a JEOL JSM 5510 scanning electron microscope equipped with an Inca X-ray microanalysis unit and applying an accelerating voltage of 20 kV.
3. µXRF maps were recorded at beamline 21, ESRF (Grenoble), using a primary beam energy of 6.57 keV, and the sample was positioned at 45° with respect to the incoming beam (0.3 x 0.8 μm^2). The fluorescence yield was recorded using a silicon drift detector at an angle of 45° with respect to the sample. A step size of 5 x 5 μm^2 was applied with a measuring time of 500 ms/pt, and all recorded spectra were evaluated using the PyMCA software package.

References

Adams and others 1997
Freddy Adams and others, "Micro and Surface Analysis in Art and Archaeology – Plenary Lecture," *Journal of Analytical Atomic Spectrometry,* v. 12, no. 3, 1997, pp. 257–265.

Bunker 1994
B.C. Bunker, "Molecular Mechanisms for Corrosion of Silica and Silicate Glasses," *Journal of Non-Crystalline Solids,* v. 179, 1994, pp. 300–308.

Cagno and others 2011
Simone Cagno and others, "Evaluation of Manganese-bodies Removal in Historical Stained Glass Windows via SR-μ-XANES/XRF and SR-μ-CT," *Journal of Analytical Atomic Spectrometry,* v. 26, no. 12, 2011, pp. 2442–2451.

Cox and Ford 1993
G.A. Cox and B.A. Ford, "The Long-term Corrosion of Glass by Groundwater," *Journal of Materials Science,* v. 28, no. 20, 1993, pp. 5637–5647.

Doménech-Carbó, Doménech-Carbó, and Osete-Cortina 2001
Antonio Doménech-Carbó, Maria-Teresa Doménech-Carbó, and Laura Osete-Cortina, "Identification of Manganese(IV) Centers in Archaeological Glass Using Microsample Coatings Attached to Polymer Film Electrodes," *Electroanalysis,* v. 13, no. 11, 2001, pp. 927–935.

Doménéch-Carbó and others 2006
Maria-Teresa Doménéch-Carbó and others, "A study on Corrosion Processes of Archaeological Glass from the Valencian Region (Spain) and its Consolidation Treatment," *Microchimica Acta,* v. 154, nos. 1–2, 2006, pp. 123–142.

Fitz 1981
Stephan Fitz, "A New Method of Cleaning Browned Medieval Glass," in *Preprints of the 6th Triennial Meeting of the ICOM Committee for Conservation*, Ottawa, 21–25 September 1981, Paris: International Council of Museums, 1981, pp. 1–6.

Fuchs, Römich, and Schmidt 1991
Dieter R. Fuchs, Hannelore Römich, and Helmut Schmidt, "Glass-Sensors: Assessment of Complex Corrosive Stresses in Conservation Research," in *Materials Issues in Art and Archaeology II*, MRS Proceedings, v. 185, Pittsburgh, PA: Materials Research Society, 1991, pp. 239–251.

Hao and others 2011
Xinli Hao and others, "Mild Aqueous Synthesis of Octahedral Mn_3O_4 Nanocrystals With Varied Oxidation States," *Colloids and Surfaces A: Physicochemical and Engineering Aspects,* v. 374, nos. 1–3, 2011, pp. 42–47.

Hind, Marsden, and Evans 1994
D. Hind, I. Marsden, and C. Evans, *Archaeological Investigations at Sidney Sussex College, Cambridge (The Dining Hall Site) 1994,* Cambridge Archaeological Unit, Report. no. 106c, 1994.

Janssens and others 1996
Koen Janssens and others, "Corrosion Phenomena in Electron, Proton and Synchrotron X-ray Microprobe Analysis of Roman Glass From Qumran, Jordan," *Nuclear Instruments & Methods in Physics Research Section B: Beam Interactions with Materials and Atoms,* v. 109, 1996, pp. 690–695.

Janssens and Van Grieken 2004
Koen Janssens and Rene Van Grieken, *Non-destructive Microanalysis of Cultural Heritage Materials, Comprehensive Analytical Chemisty*, 1st ed., 2004, Amsterdam: Elsevier.

Lopez and others 2002
Esmeralda Lopez and others, "Special Corrosion Phenomena on Glass Objects," in *First International Conference Hyalos – Vitrum – Glass: History, Technology and Conservation of Glass and Vitreous Materials in the Hellenic World*, ed. G. Kordas, Athens: Panepistemiakes Ekdoseis Phessadia, 2002, pp. 251–255.

Mees and others 2009
Florias Mees and others, "Microfocus X-ray Computed Tomography Analysis of Corroded Glass Objects," *Engineering Geology*, v. 103, nos. 3–4, 2009, pp. 93–99.

Melcher and Schreiner 2004
Michael Melcher and Manfred Schreiner, "Statistical Evaluation of Potash–lime–silica Glass Weathering," *Analytical and Bioanalytical Chemistry,* v. 379, no. 4, 2004, pp. 628–639.

Müller, Torge, and Adam 1994
Wolfgang Müller, Manfred Torge, and Karin Adam, "Ratio of CaO/K_2O >2 as Evidence of a Special Rhenish Type of Medieval Stained Glass," *Glastechnische Berichte – Glass Science and Technology,* v. 67, no. 2, 1994, pp. 45–48.

Müller, Torge, and Adam 1995
Wolfgang Müller, Manfred Torge, and Karin Adam, "Primary Stabilization Factor of the Corrosion of Historical Glasses – The Gel Layer," *Glastechnische Berichte – Glass Science and Technology,* v. 68, no. 9, 1995, pp. 285–292.

Newton and Davison 1989
Roy Newton and Sandra Davison, *Conservation of Glass,* 1997, Oxford: Butterworth–Heinemann.

Nuyts and others 2013
Gert Nuyts and others, "Study of the Early Stages of Mn Intrusion in Corroded Glass by Means of Combined SR FTIR/μXRF Imaging and XANES Spectroscopy," *Procedia Chemistry,* v. 8, 2013, pp. 239–247.

Roemich and others 2003
Hannelore Roemich and others, "Results From Burial Experiments With Simulated Medieval Glasses," *Scientific Basis for Nuclear Waste Management Xxvi,* v. 757, 2003, pp. 97–108.

Sasov and Van Dyck 1998
Alexander Sasov and Dirk Van Dyck, "Desktop X-ray Microscopy and Microtomography," *Journal of Microscopy,* v. 191, 1998, pp. 151–158.

Schalm and others 2011
Olivier Schalm and others, "Manganese Staining of Archaeological Glass: The Characterization of Mn-rich Inclusions in Leached Layers and a Hypothesis of Its Formation," *Archaeometry,* v. 53, 2011, pp. 103-122.

Scholze 1982
Horst Scholze, "Chemical Durability of Glasses," *Journal of Non-Crystalline Solids,* v. 52, nos. 1–3, 1982, pp. 91–103.

Schreiner 1991
Manfred Schreiner, "Glass of the Past – The Degradation and Deterioration of Medieval Glass Artifacts," *Mikrochimica Acta,* v. 2, nos. 1–6, 1991, pp. 255–264.

Watkinson, Weber, and Anheuser 2005
David Watkinson, L. Weber, and Killian Anheuser, "Staining of Archaeological Glass From Manganese-rich Environments," *Archaeometry,* v. 47, 2005, pp. 69–82.

Wouters 2013
Hilde Wouters, "Hidden Beauty! A New Integrated Methodology for the Evaluation of Archaeological Window Glass Collections," PhD thesis, Vrije Universiteit Brussel, Belgium, September 2013.

Authors

Gert Nuyts
University of Antwerp, Department of Chemistry, Groenenborgerlaan 171, B-2020 Antwerp, Belgium
gert.nuyts@ua.ac.be

Simone Cagno, and Koen Janssens
University of Antwerp, Department of Chemistry, Groenenborgerlaan 171, B-2020 Antwerp, Belgium

Simone Cagno
The Norwegian University of Life Sciences, Department of Plant and Environmental Sciences, P.O. Box 5003, N-1432 Ås, Norway

Jakub Jaroszewicz
Warsaw University of Technology, Department of Materials Science and Engineering, Woloska 141, 02-507, Warsaw, Poland

Hilde Wouters
Vrije Universiteit Brussel, Pleinlaan 2, B-1050 Brussels, Belgium

Kristel De Vis and Joost Caen
University of Antwerp, Faculty of Architecture and Design – Conservation Studies, Blindestraat 9, B-2000 Antwerp, Belgium

RECENT ADVANCES IN GLASS, STAINED-GLASS, AND CERAMICS CONSERVATION 2013

ICOM-CC Glass and Ceramics Working Group Interim Meeting

and

Forum of the International Scientific Committee for the Conservation of Stained Glass (Corpus Vitrearum-ICOMOS)

EDITED BY
HANNELORE ROEMICH AND
KATE VAN LOOKEREN CAMPAGNE

Spa Uitgevers

ISBN number: 978-90-8932-113-8

Publisher: SPA Uitgevers
Assendorperstraat 174-4
8012 CE Zwolle, the Netherlands
www. spa-uitgevers.nl

Layout: Hidde Heikamp, SPA publishers
Graphic design: Erica Dooijes-Hoogwijk
Proofreading: Gary Anderton (Anderton Editing),
Hoorn, the Netherlands

Editors: Hannelore Roemich and
Kate van Lookeren Campagne

Conference sponsors: Rijksmuseum, Amsterdam (RMA)
University of Amsterdam (UvA)
Cultural Heritage Agency of the Netherlands, Amsterdam (RCE)
National Museum of Antiquities, Leiden (RMO)

Cover photographs: Stained-glass panel: 'The Miracle of Amsterdam' (L. van den Essen, 1934),
Sint Franciscus Church, Bolsward, the Netherlands (Photo © Taco Hermans)
Tulip vase: Anon. 1690–1720 (in the process of conservation),
Rijksmuseum, Amsterdam, the Netherlands (Photo © Rijksmuseum)